# Determination of band offset using continuous-wave two-photon excitation in a ZnSe quantum-well waveguide structure

H. P. Wagner*
*Institut für Physik, Technische Universität Chemnitz, D-09107 Chemnitz, Germany*

M. Kühnelt
*Institut für Physik II, Universität Regensburg, D-93040 Regensburg, Germany*

H. Wenisch and D. Hommel
*Institut für Festkörperphysik, Universität Bremen, D-28334 Bremen, Germany*

(Received 5 December 2000; published 31 May 2001)

We investigate exciton subband transitions in a $ZnSe/Zn_{1-x}Mg_xS_ySe_{1-y}$ multiple-quantum-well grown by molecular beam epitaxy waveguide structure by photoluminescence excitation and two-photon excitation spectroscopy. A continuous-wave two-photon absorption is realized by an efficient waveguide coupling scheme within the cryostat. From the energetic position of the $1s$ and $2p$ exciton transitions exciton binding energies of 33 and 38 meV are deduced for heavy and light-hole excitons, respectively. With these values we are able to determine the strain free and dimensionless conduction-band-offset parameter to $Q_c = 0.3 \pm 0.1$.

DOI: 10.1103/PhysRevB.63.235319 PACS number(s): 42.50.Md, 73.21.−b, 71.35.−y, 71.55.Gs

## INTRODUCTION

The nonlinear optical method of two-photon absorption (TPA) has been widely used as powerful spectroscopic tool in quasi-two-dimensional (2D) semiconductor structures.[1–9] Depending on the optical selection rules being different from those ruling linear absorption, two-photon excitation (TPE) spectroscopy provides valuable complementary information on excited exciton states. In addition the polarization anisotropy of the dipole selection rules in quantum wells[10–17] (QW's) favors the use of planar waveguide structures in which the electric wave vector, being polarized either parallel or perpendicular to the quantum-well growth direction ($z$ axis), propagates as TE (transverse electric) or TM (transverse magnetic) mode.

While TPE on III-V semiconductor QW's was used in waveguide structures from the start of these studies,[1] most of the TPA experiments in II-VI semiconductors were performed without optical confinement due to the lack of nearly-lattice-matched systems within the class of wide-gap II-VI compounds.[6–8] Based on quaternary $Zn_xMg_{1-x}S_ySe_{1-y}$, we present results on a ZnSe multiple-QW waveguide structure grown by molecular beam epitaxy (MBE). The optical confinement together with an efficient end-fire coupling scheme within the cryostat allows the observation of two-photon exciton absorption at 12 K even with continuous-wave excitation. The combined use of photoluminescence (PL), photoluminescence excitation (PLE), and two-photon excitation (TPE) spectroscopy thus enabled us to determine the heavy-hole ($11H$) and light-hole ($11L$) exciton binding energies and to evaluate the conduction- and valence-band discontinuities in this QW structure.

## SAMPLE PREPARATION AND EXPERIMENTAL DETAILS

The $ZnSe/Zn_{1-x}Mg_xS_ySe_{1-y}$ multi-QW (MQW) waveguide structure was pseudomorphically grown by molecular beam epitaxy in an EPI twin-chamber system on a (001) GaAs substrate. Prior to growth a 200-nm-thick buffer layer was deposited on the substrate. Elemental sources for Zn, Mg, and Se were used, while sulfur was supplied by a cracker cell. The MQW structure consists of 20 nominally 4-nm-wide QW's that are separated by 20-nm-thick $Zn_{0.90}Mg_{0.10}S_{0.16}Se_{0.84}$ barriers. This structure is covered by a 2.2-$\mu$m-thick $Zn_{0.80}Mg_{0.20}S_{0.26}Se_{0.74}$ bottom layer and a 1.2-$\mu$m top layer of the same composition to enable an optical confinement of the electric light fields within the MQW structure. The uncertainty of the compositional content $x$ and $y$ is about $\pm 0.01$. More details about the MBE growth are given elsewhere.[18] The typical full width at half maximum (FWHM) in high-resolution x-ray diffraction (004 reflection) is 25 arcsec, where a superlattice period of 22.5 nm was measured, which is close to the nominal period of 24 nm. The sample was further characterized by PL and PLE measurements. In these experiments the sample was kept in a variable-temperature helium cryostat and excited by a tunable Ar-ion-laser-pumped dyelaser (Stilbene 3) at moderate excitation intensities ($I_{exc} = 1\ kW/cm^2$). The emitted signal was dispersed by a 1-m monochromator and detected by a GaAs photomultiplier.

In the TPE experiments the sample was placed in a cold-finger helium cryostat and cooled to 12 K. A high end-fire coupling efficiency was realized by using a cylindrical lens in front of the cryostat window, leading to an elliptically shaped focus that was further focused onto the entrance facet of the waveguide by a 5-nm-diam ball lens in the cryostat. A tunable Ti:sapphire laser was used as excitation source supporting a wavelength range from $\lambda = 840$ nm to 980 nm. In mode-locked operation, pulses of about 1 ps with a spectral width of 1 nm (FWHM) were provided at a repetition rate of 82 MHz. Continuous-wave operation leads to a spectral width of 0.1 nm. The average excitation power was about 0.5 W in front of the cryostat. The TPA-induced PL at the $11H$ $1s$ exciton transition was detected perpendicular to the beam

 

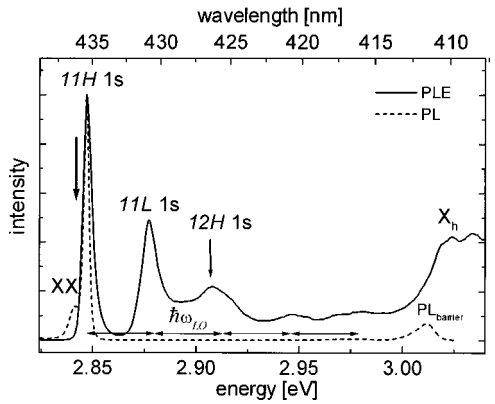


FIG. 1. PL (dashed line) and PLE (full line) spectra of a MBE-grown $ZnSe/Zn_{1-x}Mg_xS_ySe_{1-y}$ MQW waveguide structure at 10 K. The detection energy in the PLE measurements is designated by an arrow. In addition the LO-phonon energy of $\hbar\omega_{LO}=31.6$ meV is given as a double arrow for comparison.

direction ($z$ direction), where the PL signal was transferred by an optical fiber into a 46-cm grating monochromator. A charge-coupled device (CCD) array detector cooled by liquid nitrogen was used to acquire the spectral response within an integration time of typically 1 s for each excitation wavelength.

## RESULTS AND DISCUSSION

### PLE and TPE measurements

The PL spectrum of the waveguide structure at 10 K is shown in Fig. 1 as dashed line revealing a dominant signal at 2.848 eV, which is attributed to the 11$H$ 1$s$ exciton in the strained ZnSe QW. The small signal on the low-energy side of the 11$H$ exciton transition at 2.841 eV is attributed to the biexciton transition $XX$ as identified in similar structures.[19] The PL signal of the $Zn_xMg_{1-x}S_ySe_{1-y}$ barrier appears at 3.011 eV. The PLE spectrum shown as full line was recorded at a detection energy of 2.84 eV, designated by an arrow. No significant Stokes shift of the 11$H$ exciton transition is observed, indicating a weak exciton localization by QW fluctuation or interdiffusion. In addition the 11$L$ 1$s$ exciton transition is clearly detected at 2.880 eV, while the PLE signal at 2.908 eV is attributed to the 12$H$ 1$s$ exciton transition. At higher energies the PLE spectrum is governed by LO-phonon-assisted relaxation processes into the 11$H$ 1$s$ exciton state. The LO-phonon energy of $\hbar\omega_{LO}=31.6$ meV is given as a double arrow in Fig. 1 for comparison. The observed fine structure of these signals is attributed to various combinations of LO and TO phonons. It smears out when the temperature is raised to 40 K, while the line shape of the 11$L$ 1$s$ and 12$H$ 1$s$ exciton transitions remains unaffected. Finally the structure at 3.023 eV is attributed to the heavy-hole exciton transition of the barrier, the corresponding PL being Stokes shifted by 12 meV due to exciton localization caused by potential fluctuations in the quaternary material.

After adjusting and optimizing the waveguide coupling and TPE signal using picosecond excitation pulses the experiments were performed using continuous-wave excitation

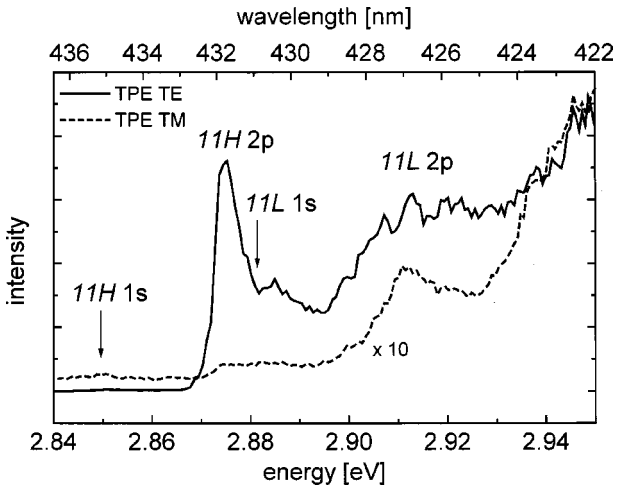


FIG. 2. Continuous-wave TPE spectra of the $ZnSe/Zn_{1-x}Mg_xS_ySe_{1-y}$ MQW waveguide structure performed with TE- (full line) an TM- (dashed line) polarized fields at 12 K. The signal obtained in TM configuration is magnified by a factor of 10 compared to the TE-TPE spectrum.

revealing a clear TPA-induced signal at the 11$H$ 1$s$ exciton transition. Small fluctuations of the laser intensity were compensated by the arithmetic mean of several measurements. Figure 2 shows the intensity-corrected TPE signal using TE (full line) and TM (dashed line) polarized fields. In the TE configuration the TPE signal was averaged from 10 single measurements, showing a clear resonance at $\lambda=431$ nm. According to the TPA dipole selection rules, which are $\Delta j=0$ for the subband transition and $\Delta l=\pm 1$ for the exciton envelope in QW's,[2] the peak at 2.879 eV is attributed to the 11$H$ 2$p$ exciton transition. For wavelengths smaller than $\lambda=429$ nm the TPA is already dominated by electron-hole contributions,[12] which are superposed by a second less pronounced and broader resonance that is assigned to the 11$L$ 2$p$ exciton transition. As expected the 11$H$ 1$s$ state, indicated by an arrow in Fig. 2, is strongly suppressed in this measurement. The small minimum on the high-energy side of the 11$H$ 2$p$ signal might be caused by a fast relaxation from the 11$H$ 2$p$ state into the 11$L$ 1$s$ state due to state mixing, thus indicating the spectrally position of the 11$L$ 1$s$ exciton state.

The TPE signal using TM polarized fields demonstrated in Fig. 2 (dashed line) shows a completely different behavior. The curve is averaged from six single measurements and the signal intensity is magnified by a factor of 10 compared to the signal obtained in the TE configuration. The TPE signal slightly increases at the 11$H$ 2$p$ resonance at $\lambda=431$ nm, which is unexpected since heavy-hole exciton states lying in the $x$-$y$ direction do not possess any dipole moment along the $z$ direction.[20] The reason for its observation is attributed to small deviations from the TM polarization possibly caused by a weak birefringence of the cryostat windows. From the dipole selection rules, which are $\Delta j=\pm 1$ for the subband transition and $\Delta l=0$ for the exciton envelope function in QW's using TM-polarized fields,[10,11] a 12$L$ 1$s$ transition is expected as the lowest observable TPE signal. From energetic reasons, however, the signal enhance-

TABLE I. Material parameters of zinc-blende crystals for calculation of QW states. In addition, the lattice constant of GaAs $a_0 = 0.56480$ nm (2 K) (Ref. 43) was used.

| | ZnSe | ZnS | MgSe |
|---|---|---|---|
| $a_0$ (nm) | 0.56596[a] (Ref. 30) | 0.54041[a] (Ref. 36) | 0.591 (Ref. 42) |
| $C_{11}$ (GPa) | 85.9 (Ref. 31) | 106.7 (Ref. 37) | 62.5 (Ref. 24) |
| $C_{12}$ (GPa) | 50.6 (Ref. 31) | 66.6 (Ref. 37) | 40.8 (Ref. 24) |
| $E_0$ (eV) | 2.8234[a] (Ref. 24) | 3.837[a] (Ref. 27) | 4.05 (Ref. 42) |
| $\Delta_{so}$ (eV) | 0.43[a] (Ref. 24) | 0.068[a] (Ref. 27) | 0.43[b] (Ref. 25) |
| $a = a_c - a_v$ (eV) | −4.9 (Ref. 32) | −5.0 (Ref. 38) | −4.2[b] (Ref. 24) |
| $b$ (eV) | −1.27 (Ref. 33) | −0.75 (Ref. 39) | −1.2[b] (Ref. 28) |
| $a_v$ (eV) | −1.0 (Ref. 32) | −1.8 (Ref. 34) | −0.5 (Ref. 28) |
| $m_c/m_0$ | 0.145 (Ref. 34) | 0.221 (Ref. 35) | 0.185 (Ref. 28) |
| $\gamma_1$ | 2.45 (Ref. 35) | 3.4 (Ref. 40) | 2.14 (Ref. 25) |
| $\gamma_2$ | 0.61 (Ref. 35) | 1.3 (Ref. 40) | 0.47 (Ref. 25) |
| $R_0$ (meV) | 20[a] (Ref. 24) | 34[a] (Ref. 41) | 57[b,c] (Ref. 25) |

[a]At 2 K.
[b]Extrapolated.
[c]Calculated.

ment at $\lambda = 427$ nm cannot be attributed to a $12L$ $1s$ transition but is again assigned to the $11L$ $2p$ transition. This transition is forbidden in pure 2D systems but weakly appears in real QW structures in which the exciton envelope has a certain extension in the $z$ direction. Since the electron–heavy-hole TPA contribution vanishes in the TM configuration due to the missing dipole moment in the $z$ direction, the energetic position of the $11L$ $2p$ transition at 2.911 eV is now clearly determinable. As discussed later the expected $12L$ $1s$ transition is already out of the tuning range of the Ti:sapphire laser but is indicated by a strong increase of the TPE signal intensity above 2.94 eV.

#### Exciton binding energy and QW band discontinuities

From the energetic differences of the $11H$ $1s$ (2.848 eV) and $11H$ $2p$ (2.875 eV) transition as well as from the $11L$ $1s$ (2.880 eV) and $11L$ $2p$ (2.911 eV) transition, which are experimentally determined with an uncertainty of $\pm 2$ meV, we are able to evaluate the fractional dimension $3 < \alpha < 2$ of the QW structure according to[21,22]

$$\frac{E_{2s} - E_{1s}}{R} = \frac{16\alpha}{(\alpha^2 - 1)^2}, \tag{1}$$

assuming equal $2p$ and $2s$ energies and with $R = 19.9$ meV being the Rydberg energy in bulk ZnSe. The resulting fractional dimensions are $\alpha(11H) = 2.55$ and $\alpha(11L) = 2.45$ for the heavy- and light-hole exciton, respectively. Using the relation[21]

$$E_n = \frac{R}{[n + (\alpha - 3)/2]^2}, \tag{2}$$

we find exciton binding energies of $E_{1s}(11H) = 33$ meV and $E_{1s}(11L) = 38$ meV. Hence the exciton binding energies exceed the LO-phonon energy of $\hbar\omega_{LO} = 31.6$ meV due to quantum confinement, a fact that cannot be achieved in GaAs-based QW structures. The higher binding energy of the light-hole exciton is thereby explained by the higher effective in-plane mass.

With the knowledge of these exciton binding energies we are able to deduce the $11H$ and $11L$ subband transition energies, which we can compare with calculated values based on the envelope function approximation[23] in which heavy- and light-hole excitons are considered to be decoupled. Hence we can evaluate the QW band discontinuities that are determined by the strain-free and dimensionless conduction-band-offset parameter

$$Q_c = \frac{V_c(\epsilon) + \delta E_c^w(\epsilon) - \delta E_c^b(\epsilon)}{E_0^b - E_0^w}, \tag{3}$$

as outlined in Refs. 24 and 25, where $V_c(\epsilon)$ is the strain-dependent conduction-band offset, and $E_0^b$ and $E_0^w$ are the gap energies of the unstrained barrier and well material. $\delta E_c^b(\epsilon)$ and $\delta E_c^w(\epsilon)$ are the absolute strain-dependent shifts of the conduction bands of the barrier and well, respectively. The used material parameters for these calculations are given in Table I. Since no reliable experimental values are available for cubic MgS so far [with the exception of the lattice constant, which is $a_{MgS} = 0.562$ nm at 300 K (Ref. 26)] the parameters of the quaternary $Zn_{1-x}Mg_xS_ySe_{1-y}$ barrier were deduced from the data of ZnSe, ZnS, and MgSe alone. In the case of $ZnS_ySe_{1-y}$ a bowing of the valence and the split-off band
[$b_0 = 0.51$ eV, $b_{so} = -0.22$ eV (Ref. 27)] was considered whereas a linear increase of the gap energy was assumed for $Zn_{1-x}Mg_xSe$. The gap energy of the unstrained barrier $E_0^b$ thus reads

$$E_0^b = E_0^{ZnSe} + y(E_0^{ZnS} - E_0^{ZnSe} - b_0) + b_0 y^2 + x(E_0^{MgSe} - E_0^{ZnSe}). \tag{4}$$

The unstrained barrier lattice constant $a_0^b$ was determined according to

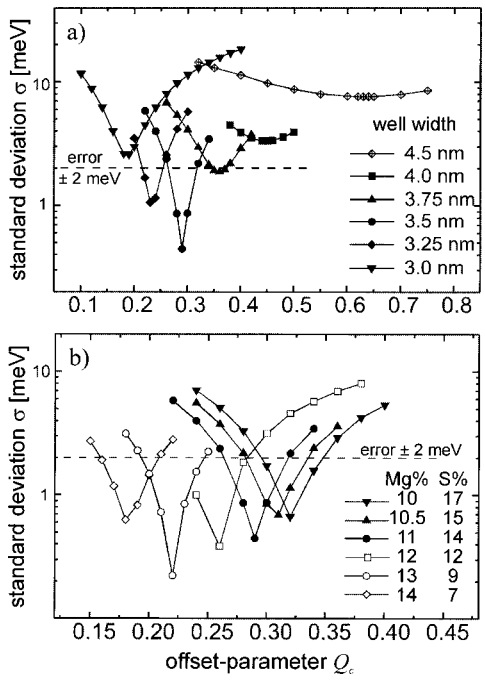


FIG. 3. (a) Variation of the strain-free and dimensionless conduction-band-offset parameter $Q_c$ for various well widths in which a $Zn_{0.89}Mg_{0.11}S_{0.14}Se_{0.86}$ barrier was used and (b) for different compositional content using a QW width of 3.5 nm. The dashed line gives the experimental error value. The open symbols in (b) indicate compositional content for which lattice-matched growth is not possible.

$$a_0^b=(1-x)(1-y)a_0^{\mathrm{ZnSe}}+x(1-y)a_0^{\mathrm{MgSe}}+y(1-x)a_0^{\mathrm{ZnS}}+xya_0^{\mathrm{MgS}}, \tag{5}$$

where a lattice constant of $a_{\mathrm{MgS}}(2\,\mathrm{K})=0.560\,\mathrm{nm}$ was deduced from the 300 K value assuming a similar temperature dependence as in ZnS. The remaining parameters $P$ were estimated according to the relation

$$P^b=P^{\mathrm{ZnSe}}+x(P^{\mathrm{MgSe}}-P^{\mathrm{ZnSe}})+y(P^{\mathrm{ZnS}}-P^{\mathrm{ZnSe}}). \tag{6}$$

The resulting barrier parameters, e.g., the band gap $E_0^b$ or the lattice constant $a_0^b$, are in good agreement with the experimental data obtained from PL and x-ray measurements. The best agreement was found using a Mg and S content of $x=0.11$ and $y=0.14$, respectively, which is close to the nominal values.

The only free parameter in our model is therefore $Q_c$, which is determined by the minimum mean standard deviation $\sigma$ between calculated and experimental $11H$ and $11L$ transition energies:

$$\sigma=\left(\frac{1}{N}\sum_{i=1}^{N}(\Delta E_i^{\mathrm{expt}}-\Delta E_i^{\mathrm{calc}})^2\right)^{1/2}. \tag{7}$$

Since the transition energies of QW states are extremely sensitive to the QW width, we varied the well width in our calculations using $x=0.11$ and $y=0.14$. Figure 3(a) demonstrates that the experimental data cannot be reproduced within the experimental error of 2 meV using a 4-nm-wide QW. Better agreement is found using smaller QW's where the variation of $Q_c$ reveals a pronounced minimum using a QW size of 3.5 nm. The smaller well width is in accordance with x-ray measurement, providing a shorter superlattice period than nominally expected. The optimal fit reveals at a value of $Q_c=0.3$.

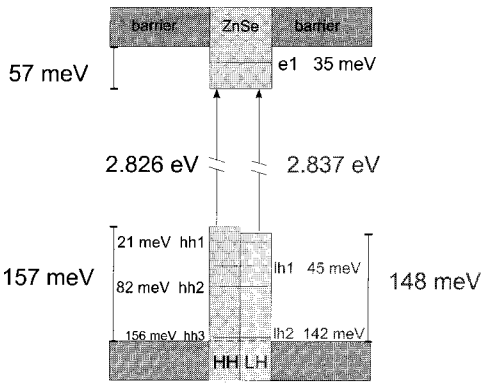


FIG. 4. Calculated absolute subband energies in a $Zn_{0.89}Mg_{0.11}S_{0.14}Se_{0.86}/ZnSe$ MQW structure, using an offset parameter of $Q_c=0.3$.

Finally, the composition of the quaternary barrier was varied, showing a less effective influence on the mean standard deviation $\sigma$. Figure 3(b) gives the data for a varying $Q_c$ and various Mg and S contents as labeled. In all cases the agreement is better than the experimental uncertainty. At higher Mg content the value of $Q_c$ tends to values below 0.2 while a higher S content leads to values above 0.3. This result is in agreement with the experimentally found values of $Q_c=0.13$ reported from $Zn_{1-x}Mg_xSe/ZnSe$ QW structures[25] and $Q_c=0.35$ found in $ZnS_ySe_{1-y}/ZnSe$ QW's.[29] The deduced value of $Q_c=0.3$ in the investigated $Zn_{1-x}Mg_xS_ySe_{1-y}/ZnSe$ MQW structure nicely fits between these values. It should be noted that Mg content above $x>0.11$ prevents a pseudomorphic growth above a 1-$\mu$m layer thickness. These data are therefore given as open symbols in Fig. 3(b).

From the performed variational calculations an error of $Q_c$ of about $\pm 0.03$ can be deduced. Uncertainties of the quaternary material parameters as well as approximating assumptions in the used model, however, prompted us to declare an error of about $\pm 0.1$.

The absolute subband energies in a $Zn_{0.89}Mg_{0.11}S_{0.14}Se_{0.86}/ZnSe$ QW, which are summarized in Fig. 4, are calculated as follows: The QW band edges are $E_{\mathrm{HH}}^w=2.826\,\mathrm{eV}$ and $E_{\mathrm{LH}}^w=2.837\,\mathrm{eV}$ and the discontinuities are $V_c=57\,\mathrm{meV}$, $V_{\mathrm{HH}}=157\,\mathrm{meV}$, and $V_{\mathrm{LH}}=148\,\mathrm{meV}$. Therefore only 27% and 28% of the gap energy contribute to the conduction-band discontinuity. This result is in contrast to the common anion/cation rule, which predicts a conduction-band offset of about 60% of the gap energy.[44,45] However, this rule already failed for ternary $Zn_{1-x}Mg_xSe/ZnSe$ (Ref. 25) and $ZnS_ySe_{1-y}/ZnSe$ (Ref. 29) QW systems, and our value of $Q_c=0.3\pm 0.1$ is supported by investigations of other groups[46–48] with values in the range $0.1<Q_c<0.4$ using various $Zn_{1-x}Mg_xS_ySe_{1-y}$ systems. Finally, the energetic positions of the electron and various HH

and LH subband states are given in Fig. 4. The calculations predict a $12H$ $1s$ transition at 2.910 eV (assuming an exciton binding energy of 33 meV), which is in good agreement with the experimental value of 2.908 eV obtained from the PLE measurements. Furthermore a $12L$ $1s$ exciton transition is expected at about 2.975 eV, which might be indicated by a small peak in the PLE measurements at slightly lower energies.

## CONCLUSIONS

We have performed PL, PLE, and TPE measurements on a MBE-grown $Zn_{0.89}Mg_{0.11}S_{0.14}Se_{0.86}/ZnSe$ MQW waveguide structure. The high $\chi^{(3)}$ nonlinearity in II-VI materials and an efficient coupling scheme within the cryostat enabled us to perform TPA measurement with high spectral resolution using continuous-wave excitation. From the energetic positions of the $11H$ $1s$ and $11L$ $1s$ transitions provided by PLE and the $11H$ $2p$ and $11L$ $2p$ transitions obtained from TPE we were able to deduce the exciton binding energies using the model of fractional dimension. The evaluated values of $E_{1s}(11H)=33\,\mathrm{meV}$ and $E_{1s}(11L)=38\,\mathrm{meV}$ for heavy and light-hole excitons, respectively, exceed the LO-phonon energy and might lead to a modified exciton–LO-phonon scattering, which will be the subject of a forthcoming work. A comparison of $11H$ and $11L$ subband transition energies with calculated values further enabled us to determine the value of the strain-free and dimensionless conduction-band parameter $Q_c$. The low value of $Q_c=0.3\pm0.1$ is in contrast to the common anion rule but is supported by investigations of several other groups, thus justifying the reliability of the used model calculations.

## ACKNOWLEDGMENTS

The experimental support of W. Langbein and H.-P. Tranitz are kindly acknowledged.

*Author to whom correspondence should be addressed. Electronic address: hp.wagner@physik.tu-chemnitz.de

[1] K. Tai, A. Mysyrowicz, R. J. Fischer, R. E. Slusher, and A. Y. Cho, Phys. Rev. Lett. **62**, 1784 (1989).
[2] I. M. Catalano, A. Cingolani, M. Lepore, R. Cingolani, and K. Ploog, Solid State Commun. **71**, 217 (1989).
[3] I. M. Catalano, A. Cingolani, R. Cingolani, M. Lepore, and K. Ploog, Phys. Rev. B **40**, 1312 (1989).
[4] K. Fujii, A. Shimizu, J. Bergquist, and T. Sawada, Phys. Rev. Lett. **65**, 1808 (1990).
[5] C. C. Yang, A. Villeneuve, G. I. Stegeman, C.-H. Lin, H.-H. Lin, IEEE J. Quantum Electron. **29**, 2934 (1993).
[6] M. Lepore, M. C. Netti, R. Tommasi, I. M. Catalano, and I. Suemune, Solid State Commun. **92**, 695 (1994).
[7] F. Minami, K. Yoshida, K. Inoue, and H. Fujiyasu, J. Cryst. Growth **139**, 796 (1994).
[8] M. C. Netti, M. Lepore, A. Adinolfi, A. Tommasi, I. M. Catalano, L. Vanzetti, L. Sorba, and A. Franciosi, J. Appl. Phys. **80**, 2908 (1996).
[9] M. Lepore, A. Adinolfi, M. C. Netti, I. Catalano, and I. Suemune, J. Phys.: Condens. Matter **9**, 7667 (1997).
[10] H. N. Spector, Phys. Rev. B **35**, 5876 (1987).
[11] A. Pasquarello, A. Quadropani, Phys. Rev. B **38**, 6206 (1988).
[12] A. Shimizu, Phys. Rev. B **40**, 1403 (1989).
[13] A. Pasquarello and A. Quadropani, Phys. Rev. B **41**, 12728 (1990).
[14] A. Pasquarello and A. Quadropani, Phys. Rev. B **42**, 9073 (1990).
[15] A. Shimizu, T. Ogawa, and H. Sakaki, Surf. Sci. **263**, (1992).
[16] A. Obeidat and J. Khurgin, J. Opt. Soc. Am. B **12**, 1222 (1995).
[17] S. K. Avetissian, A. O. Melikan, and H. R. Minassian, J. Appl. Phys. **80**, 301 (1996).
[18] P. Michler, M. Vehse, J. Gutowski, M. Behringer, D. Hommel, M. P. Pereira, and K. Henneberger, Phys. Rev. B **58**, 2055 (1998).
[19] O. Homburg, P. Michler, R. Heinecke, J. Gutowski, H. Wenisch, M. Behringer, and D. Hommel, Phys. Rev. B **60**, 5743 (1999).
[20] *Fundamentals of Semiconductors*, edited by P. Y. Yu and M. Cardona (Springer Berlin, 1996).
[21] X. F. He, Phys. Rev. B **43**, 2063 (1991).
[22] G. Bastard, A. A. Brum, and R. Ferreira, Solid State Phys. **44**, 229 (1991).
[23] H. Mathieu, P. Levebv, and P. Christol, Phys. Rev. B **46**, 4092 (1992).
[24] M. Wörz, E. Griebl, Th. Reisinger, B. Flierl, D. Haserer, T. Semmler, T. Frey, and W. Gebhardt, Phys. Status Solidi B **202**, 805 (1997).
[25] E. Griebl, A. Stier, M. Krenzer, M. Krenzer, T. Reisinger, H. Preis, and W. Gebhardt, J. Cryst. Growth **184/185**, 853 (1998).
[26] H. Okuyama, Y. Kishita, and A. Ishibashi, Phys. Rev. B **57**, 2257 (1998).
[27] Gerhard Schötz, Ph.D. thesis, Universität Regensburg, 1995.
[28] Erich Griebl, Ph.D. thesis, Universität Regensburg, 1998.
[29] Simon Lankes, Ph.D. thesis, Universität Regensburg, 1995.
[30] B. Seagull and D. T. F. Marple, in *Physics and Chemistry of II-VI Compounds*, edited by M. Aven and J. S. Prener (North Holland, Amsterdam, 1967).
[31] B. H. Lee, J. Appl. Phys. **41**, 2988 (1970).
[32] G. F. Schötz, W. Sedlmeier, M. Lindner, and W. Gebhardt, J. Phys.: Condens. Matter **7**, 795 (1995).
[33] Y. R. Lee, A. K. Ramdas, L. A. Kolodziejski, and R. L. Gunshor, Phys. Rev. B **38**, 13 143 (1988).
[34] N. Miura and Y. Imanaka *II-VI-Compounds and Semimagnetic Semiconductors*, Material Sci. Forum No. 182–184 (Trans Tech, Switzerland, 1994).
[35] H. W. Hölscher, A. Nöthe, and C. Uihlein, Phys. Rev. B **31**, 2379 (1985).
[36] R. R. Reeber, Phys. Status Solidi A **32**, 321 (1975).
[37] R. B. Hall and J. D. Meakin, Thin Solid Films **63**, 203 (1979).
[38] S. Ves, U. Schwarz, N. E. Christensen, K. Syassen, and M. Cardona, Phys. Rev. B **42**, 9113 (1990).
[39] A. Blacha, H. Presting, and M. Cardona, Phys. Status Solidi B **126**, 11 (1984).
[40] P. Lawaetz, Phys. Rev. B **4**, 3460 (1971).
[41] A. Mang, K. Reimann, and S. Rübenacke, Solid State Commun. **94**, 251 (1995).

[42] B. Jobst, D. Hommel, U. Lunz, T. Gerhard, G. Landwehr, Appl. Phys. Lett. **69**, 97 (1996).
[43] ''Thermophysical properties of matter,'' edited by Y. S. Touloukian (Plenum, New York, 1975), Vols. 12 and 13.
[44] J. Suda, Y. Kawakami, Sz. Fujita, Sg. Fujita, Jpn. J. Appl. Phys., Part 2 **33**, L986 (1994).
[45] J. Suda, M. Ogawa, K. Sakurai, Y. Kawakami, Sz. Fujita, and Sg. Fujita, J. Cryst. Growth **184/185**, 863 (1998).
[46] K. Shahzad, J. Petruzzello, J. M. Gaines, and C. Ponzoni, Appl. Phys. Lett. **67**, 659 (1995).
[47] T. Miyajima, F. P. Logue, J. F. Donegan, J. Hegarty, H. Okuyama, A. Ishibashi, and Y. Mori, Appl. Phys. Lett. **66**, 180 (1995).
[48] H. Hamdeh, M. Lünenbürger, H. Kalisch, and M. Heuken, J. Cryst. Growth **184/185**, 867 (1998).